PCCP

ROYAL SOCIETY OF CHEMISTRY

PAPER

View Article Online
View Journal | View Issue

Cite this: *Phys. Chem. Chem. Phys.*, 2022, **24**, 7045

Low-energy Ga_2O_3 polymorphs with low electron effective masses†

Qingyang Fan, *[ab] Ruida Zhao,[a] Wei Zhang,[c] Yanxing Song,[c] Minglei Sun[d] and Udo Schwingenschlögl *[d]

Received 17th November 2021,
Accepted 22nd February 2022

DOI: 10.1039/d1cp05271c

rsc.li/pccp

We predict three Ga_2O_3 polymorphs with $P2_1/c$ or *Pnma* symmetry. The formation energies of $P2_1/c$ Ga_2O_3, *Pnma*-I Ga_2O_3, and *Pnma*-II Ga_2O_3 are 57 meV per atom, 51 meV per atom, and 23 meV per atom higher than that of β-Ga_2O_3, respectively. All the polymorphs are shown to be dynamically and mechanically stable. $P2_1/c$ Ga_2O_3 is a quasi-direct wide band gap semiconductor (3.83 eV), while *Pnma*-I Ga_2O_3 and *Pnma*-II Ga_2O_3 are direct wide band gap semiconductors (3.60 eV and 3.70 eV, respectively). Simulated X-ray diffraction patterns are provided for experimental confirmation of the predicted structures. The polymorphs turn out to provide low electron effective masses, which is of great benefit to high-power electronic devices.

Introduction

Wide band gap semiconductors are important for devices requiring high frequency, temperature, and/or power.[1] Many commercial applications use the third generation semiconductors GaN and SiC. However, those suffer from high manufacturing costs and limitations of the achievable performance.[2,3]

Gallium oxide, especially thermodynamically stable β-Ga_2O_3, attracts more and more attention, because its high breakdown field leads to a higher Baliga figure of merit for application in high-power electronic devices than provided by SiC and GaN.[4] The most famous polymorphs of Ga_2O_3 are the α-, β-, γ-, δ-, and ε-phases,[5,6] which are similar in properties such as the band gap, elastic modulus, and electron effective mass.[7] The hexagonal structure of ε-Ga_2O_3 with space group $P6_3mc$ enables heteroepitaxial growth on GaN, AlN, ZnO, and Al_2O_3.[8] While theoretical studies focus on the orthorhombic $Pna2_1$ phase,[7,9–12] experiments show that ε-Ga_2O_3 is pyroelectric with large polarization and piezoelectric coupling, being able to host a high density electron gas. Various theoretical studies address the physical properties of the β-phase and experimental studies the preparation of non-β-phases.[12–25]

In the present work, we predict three Ga_2O_3 polymorphs, which we call $P2_1/c$ Ga_2O_3, *Pnma*-I Ga_2O_3, and *Pnma*-II Ga_2O_3 according to their space groups. The formation energy of *Pnma*-II Ga_2O_3 is found to be 3 meV per atom lower than that of α-Ga_2O_3. A systematic investigation of the predicted polymorphs is performed, including the stability, electronic states, and carrier effective mass.

Computational details

Based on density functional theory, all calculations are performed with the Cambridge Serial Total Energy Package.[26] We use the generalized gradient approximation of Perdew–Burke–Ernzerhof for structure optimization and the Heyd–Scuseria–Ernzerhof hybrid functional for calculating electronic properties. Ultrasoft pseudopotentials[27] and the Broyden–Fletcher–Goldfarb–Shanno scheme are adopted. Brillouin zone integrations are performed on Monkhorst–Pack 8 × 5 × 14, 6 × 12 × 4, and 7 × 13 × 3 *k*-grids for $P2_1/c$ Ga_2O_3, *Pnma*-I Ga_2O_3, and *Pnma*-II Ga_2O_3, respectively. Elastic constants are calculated by the strain-stress method. Phonon spectra are obtained by density functional perturbation theory.[28]

Results and discussion

The crystal structures of the predicted Ga_2O_3 polymorphs are shown in Fig. 1. In each case the unit cell contains 8 Ga and 12 O atoms. In $P2_1/c$ Ga_2O_3 and *Pnma*-I Ga_2O_3 the Ga atoms are 4- or 5-coordinated and the O atoms are 3-coordinated, whereas in *Pnma*-II Ga_2O_3 the Ga atoms are 4- or 6-coordinated and the O atoms are 3-coordinated (α-Ga_2O_3: O atoms 4-coordinated

[a] *College of Information and Control Engineering, Xi'an University of Architecture and Technology, Xi'an 710055, China*
[b] *Shaanxi Key Laboratory of Nano Materials and Technology, Xi'an, 710055, China. E-mail: fanqy@xauat.edu.cn*
[c] *School of Microelectronics, Xidian University, Xi'an 710071, China*
[d] *Applied Physics Program, Physical Science and Engineering Division, King Abdullah University of Science and Technology (KAUST), Thuwal 23955-6900, Saudi Arabia. E-mail: udo.schwingenschlogl@kaust.edu.sa*

† Electronic supplementary information (ESI) available. See DOI: 10.1039/d1cp05271c

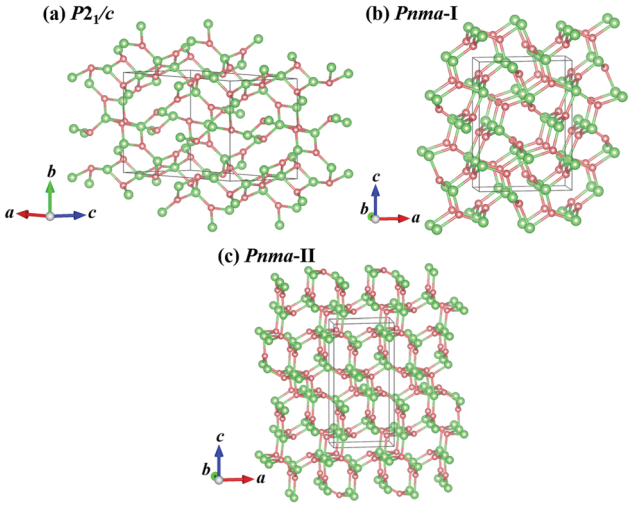

Fig. 1 Crystal structures. Red spheres represent O atoms and green spheres represent Ga atoms.

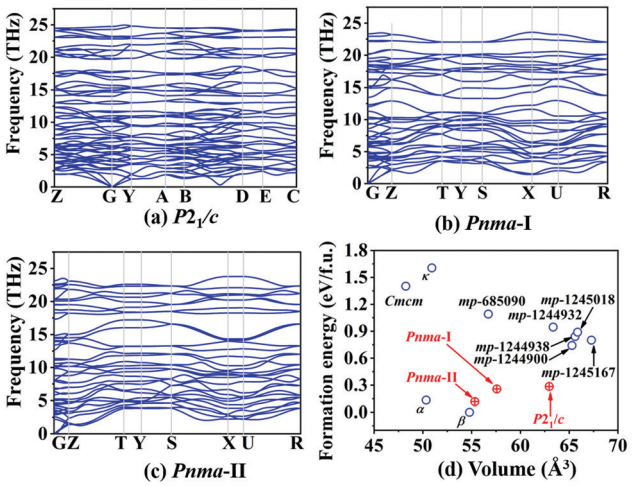

Fig. 2 (a–c) Phonon spectra. (d) Formation energies with respect to β-Ga_2O_3.

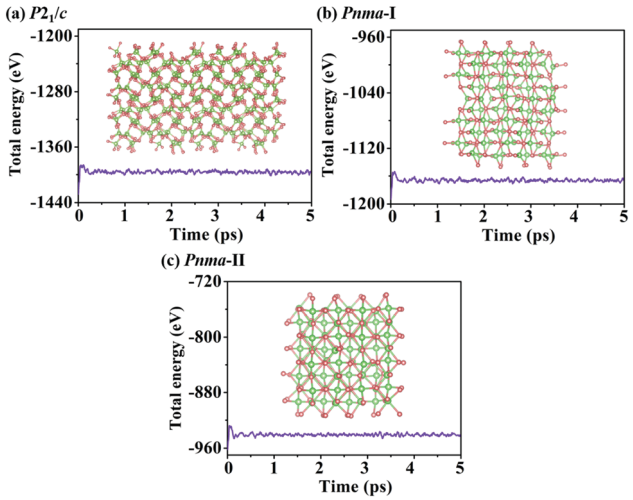

Fig. 3 *Ab initio* molecular dynamics simulations at 1000 K: total energy and final structures.

and Ga atoms 6-coordinated; β-Ga_2O_3: O atoms 3- or 4-coordinated and Ga atoms 4- or 6-coordinated). The lattice parameters of the predicted polymorphs are compared to those of α-Ga_2O_3 and β-Ga_2O_3 in Table 1. The theoretical values of α-Ga_2O_3 and β-Ga_2O_3 show excellent agreement with the experiment (deviation less than 1.8%), demonstrating reliability of the employed theoretical methodology. The densities of the predicted polymorphs are smaller than those of α-Ga_2O_3 and β-Ga_2O_3.

The phonon spectra of the predicted polymorphs are shown in Fig. 2. Absence of imaginary frequencies indicates dynamical stability. Fig. 2(d) gives the formation energies of selected polymorphs with respect to that of β-Ga_2O_3 (minimum). The values of the predicted polymorphs are much lower than those of polymorphs from the Materials Project (mp). We calculate for mp-13134 a value of 280 meV per atom in agreement with the mp-result of 284 meV per atom. The formation energies of $P2_1/c$ Ga_2O_3, *Pnma*-I Ga_2O_3, and *Pnma*-II Ga_2O_3 are only moderately higher (57 meV per atom, 51 meV per atom, and 23 meV per atom, respectively) than that of β-Ga_2O_3. The formation energy of *Pnma*-II Ga_2O_3 is even 3 meV per atom lower than that of α-Ga_2O_3. To verify the stability of the predicted polymorphs at operating temperature, *ab initio* molecular dynamics simulations are performed at 1000 K (5 ps with a time step of 1 fs). The results in Fig. 3 show no indication of structural instability.

The elastic matrix of monoclinic $P2_1/c$ Ga_2O_3 has 13 independent constants and the elastic matrices of orthorhombic *Pnma*-I and *Pnma*-II Ga_2O_3 have 9 independent constants. The obtained elastic matrices and the Born mechanical stability conditions are given in the ESI† material. The elastic constants in Table 2 show that the Born mechanical stability criteria are fulfilled for all the predicted polymorphs. The bulk modulus B, shear modulus G, and Young's modulus E of *Pnma*-II Ga_2O_3 are found to resemble the values of β-Ga_2O_3 (Table 2).

The obtained electronic band structures in Fig. 4 show a quasi-direct band gap for $P2_1/c$ Ga_2O_3 (3.83 eV) and direct band

Table 1 Lattice parameters and densities

Ga_2O_3		a (Å)	b (Å)	c (Å)	β (°)	ρ (g cm^{-3})
α	Theory	4.988		13.625		6.46
	Exp.[29]	4.983		13.433		6.47
β	Theory	12.452	3.083	5.876	103.7	5.68
	Exp.[30]	12.230	3.040	5.800	103.7	5.94
$P2_1/c$	Theory	9.770	8.762	5.810	149.6	4.95
Pnma-I	Theory	7.073	3.311	9.835		5.41
Pnma-II	Theory	5.900	3.093	12.126		5.63

Table 2 Elastic constants (GPa) and moduli (GPa)

Ga_2O_3	C_{11}	C_{22}	C_{33}	C_{44}	C_{55}	C_{66}	C_{12}	C_{13}	C_{23}	B	G	E
α	365	365	327	75	75	108	149	106	106	197	96	248
β	199	312	298	39	77	95	112	125	62	155	69	180
$P2_1/c$	175	253	204	45	59	47	62	66	88	116	53	138
Pnma-I	210	269	257	53	73	51	90	109	122	152	62	164
Pnma-II	311	300	193	81	96	41	59	116	120	154	71	185

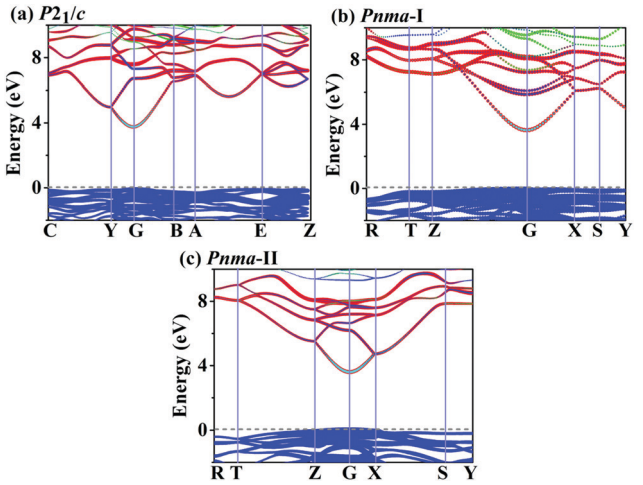

Fig. 4 Electronic band structures. Red, green, cyan, and blue colors represent Ga s, Ga p, O s, and O p contributions, respectively. The high symmetry points are *C* (0.0, 0.5, 0.5), *Y* (0.0, 0.5, 0.0), *G* (0.0, 0.0, 0.0), *B* (0.5, 0.0, 0.0), *A* (0.5, 0.5, 0.0), *E* (0.5, 0.5, 0.5), and *Z* (0.0, 0.0, 0.5) for $P2_1/c$ symmetry and *R* (−0.5, 0.5, 0.5), *T* (−0.5, 0.0, 0.5), *Z* (0.0, 0.0, 0.5), *G* (0.0, 0.0, 0.0), *X* (0.0, 0.5, 0.0), *S* (−0.5, 0.5, 0.0), and *Y* (−0.5, 0.0, 0.0) for *Pnma* symmetry.

gaps for *Pnma*-I Ga_2O_3 (3.60 eV) and *Pnma*-II Ga_2O_3 (3.70 eV). Although these band gaps are smaller than that of β-Ga_2O_3 (4.60 eV),[31] they exceed those of SiC (2.40 eV), GaN (3.20 eV), and ZnO (3.44 eV).[32] Note that the calculated band gap of β-Ga_2O_3 is 4.60 eV, in perfect agreement with the experimental result of ref. 31.

We present the calculated electron and hole effective masses along the *a*-, *b*-, and *c*-axes in Table 3. The electron effective masses of *Pnma*-I Ga_2O_3 are similar to those of α-Ga_2O_3 and β-Ga_2O_3, those of $P2_1/c$ Ga_2O_3 are a bit larger, and those of *Pnma*-II Ga_2O_3 are significantly larger by a factor of almost 2.5. We find hardly any anisotropy for the electron effective masses. For $P2_1/c$ Ga_2O_3 the minimum appears not in a special direction, for *Pnma*-I Ga_2O_3 it appears along the *a*-axis, and for *Pnma*-II Ga_2O_3 it appears along the *b*-axis. The hole effective masses show significant anisotropy. For both $P2_1/c$ Ga_2O_3 and *Pnma*-II Ga_2O_3 the minimum appears along the *b*-axis and for *Pnma*-I Ga_2O_3 it appears along the *c*-axis. $P2_1/c$ Ga_2O_3 and *Pnma*-II Ga_2O_3 show heavy fermion behavior in specific directions (Table 3).

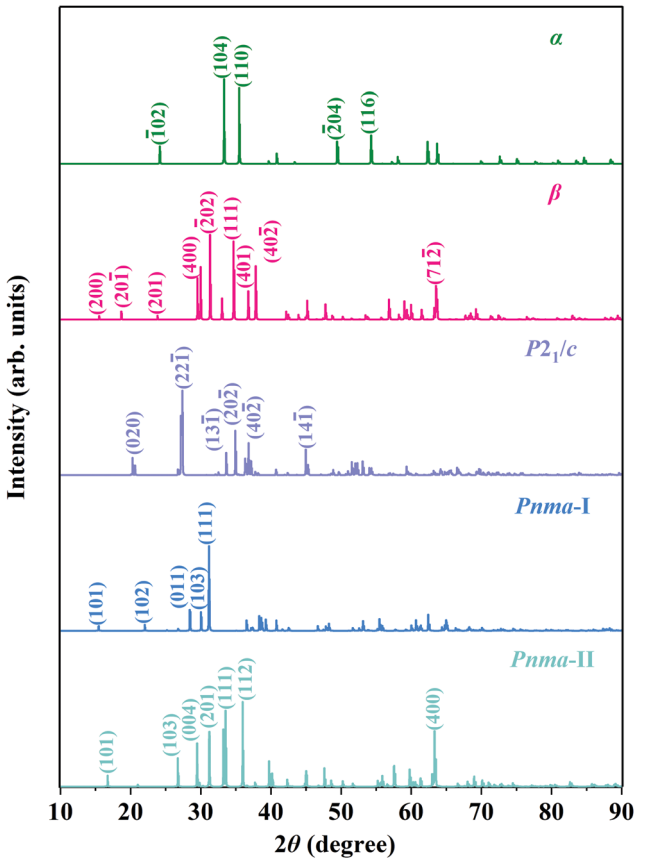

Fig. 5 X-Ray diffraction patterns (Cu source with a wavelength of 1.5406 Å).

The simulated X-ray diffraction patterns of α-Ga_2O_3, β-Ga_2O_3, $P2_1/c$ Ga_2O_3, *Pnma*-I Ga_2O_3, and *Pnma*-II Ga_2O_3 are displayed in Fig. 5. The (111) and (400) peaks of β-Ga_2O_3 (at 34.7° and 29.5°, respectively) coincide with the mp-results. Though they belong to the same space group, the spectra of *Pnma*-I Ga_2O_3 and *Pnma*-II

Table 3 Electron and hole effective masses (multiples of the free electron mass)

		Electron effective mass					
Ga_2O_3	m_a	m_b	m_c	m_{max}	Direction	m_{min}	Direction
α	0.21	0.21	0.21	0.21	[1, 1, 1]	0.21	[1, 1, 1]
β	0.22	0.22	0.21	0.23	[0.68, −0.73, 0.02]	0.21	[−0.22, −0.22, 0.95]
$P2_1/c$	0.26	0.26	0.26	0.26	[0, 1, 0]	0.26	[−0.62, 0, 0.78]
Pnma-I	0.20	0.23	0.23	0.23	[0, 1, 0]	0.20	[1, 0, 0]
Pnma-II	0.51	0.51	0.54	0.54	[0, 0, 1]	0.51	[0, 1, 0]
		Hole effective mass					
Ga_2O_3	m_a	m_b	m_c	m_{max}	Direction	m_{min}	Direction
α	2.54	2.54	0.80	3.47	[0.67, 0.67, 0.31]	0.71	[0.25, 0.25, 0.93]
β	2.81	3.49	4.54	6.06	[0.25, 0.56, 0.79]	2.57	[−0.85, −0.53, 0.04]
$P2_1/c$	2.55	2.26	5.03	>50	[−0.56, 0, 0.83]	2.26	[0, 1, 0]
Pnma-I	2.29	2.29	0.31	2.29	[1, 0, 0]	0.31	[0, 0, 1]
Pnma-II	4.07	0.37	>50	>50	[0, 0, 1]	4.07	[0, 1, 0]

Ga_2O_3 reveal notable differences. The strongest peaks are (22–1) at 27.3° for $P2_1/c$ Ga_2O_3, (111) at 33.5° for *Pnma*-I Ga_2O_3, and (112) at 35.9° for *Pnma*-II Ga_2O_3. The X-ray characteristics enable identification of the predicted polymorphs in future experiments.

Conclusions

In conclusion, three low-energy Ga_2O_3 polymorphs with wide band gaps are predicted to be dynamically and mechanically stable. $P2_1/c$ Ga_2O_3 and *Pnma*-I Ga_2O_3 realize a novel 5-coordination of the Ga atoms. The band gap is quasi-direct for $P2_1/c$ Ga_2O_3 and direct for *Pnma*-I Ga_2O_3 and *Pnma*-II Ga_2O_3. The electron and hole effective masses show significant differences from those of α-Ga_2O_3 and β-Ga_2O_3. Simulated X-ray diffraction patterns enable experimental confirmation of the predicted structures. Remarkably, chemical vapor deposition can be used to synthesize a large variety of Ga_2O_3 polymorphs, adopting temperatures of 410 °C,[33] 550 °C,[34] and 650 °C.[35] When aiming for synthesis of the predicted polymorphs by this method, identifying a suitable growth temperature is the main experimental uncertainty. However, since structural stability is maintained beyond 1000 K, it is reasonable to expect that appropriate growth parameters can be established.

Data availability statement

The data that supports the findings of this study are available within the article and its supplementary material.

Conflicts of interest

The authors have no conflicts to disclose.

Acknowledgements

The authors acknowledge generous financial support from the National Natural Science Foundation of China (No. 61804120), China Postdoctoral Science Foundation (No. 2019TQ0243 and 2019M663646), Key Scientific Research Plan of the Education Department of Shaanxi Province (Key Laboratory Project) (No. 20JS066), and Young Talent Fund of the University Association for Science and Technology in Shaanxi, China (No. 20190110). The research reported in this publication was supported by funding from King Abdullah University of Science and Technology (KAUST).

References

1 C. G. Van de Walle, *Wide-band-gap semiconductors*, Elsevier, Amsterdam, 2012.
2 W. Kowbel, C. A. Bruce, K. L. Tsou, K. Patel, J. C. Withers and G. E. Youngblood, High thermal conductivity SiC/SiC composites for fusion applications, *J. Nucl. Mater.*, 2000, **283–287**, 570–573.
3 J. Kim, D. Tahara, Y. Miura and B. G. Kim, First-principle calculations of electronic structures and polar properties of (κ,ε)-Ga_2O_3, *Appl. Phys. Express*, 2018, **11**, 061101.
4 M. Higashiwaki, K. Sasaki, H. Murakami, Y. Kumagai, A. Koukitu, A. Kuramata, T. Masui and S. Yamakoshi, Recent progress in Ga_2O_3 power devices, *Semicond. Sci. Technol.*, 2016, **31**, 034001.
5 R. Roy, V. G. Hill and E. F. Osborn, Polymorphism of Ga_2O_3 and the system Ga_2O_3–H_2O, *J. Am. Chem. Soc.*, 1952, **74**, 719–722.
6 J. Furthmüller and F. Bechstedt, Quasiparticle bands and spectra of Ga_2O_3 polymorphs, *Phys. Rev. B*, 2016, **93**, 115204.
7 S. Yoshioka, H. Hayashi, A. Kuwabara, F. Oba, K. Matsunaga and I. Tanaka, Structures and energetics of Ga_2O_3 polymorphs, *J. Phys.: Condens. Matter*, 2007, **19**, 346211.
8 H. Y. Playford, A. C. Hannon, E. R. Barney and R. I. Walton, Structures of uncharacterised polymorphs of gallium oxide from total neutron diffraction, *Chem. – Eur. J.*, 2013, **19**, 2803–2813.
9 I. Cora, F. Mezzadri, F. Boschi, M. Bosi, M. Čaplovicová, G. Calestani, I. Dodony, B. Pecz and R. Fornari, The real structure of ε-Ga_2O_3 and its relation to κ-phase, *CrystEngComm*, 2017, **19**, 1509–1516.
10 M. B. Maccioni and V. Fiorentini, Phase diagram and polarization of stable phases of $(Ga_{1-x}In_x)_2O_3$, *Appl. Phys. Express*, 2016, **9**, 041102.
11 M. Kracht, A. Karg, J. Schörmann, M. Weinhold, D. Zink, F. Michel, M. Rohnke, M. Schowalter, B. Gerken, A. Rosenauer, P. J. Klar, J. Janek and M. Eickhoff, Tin-assisted synthesis of ε-Ga_2O_3 by molecular beam epitaxy, *Phys. Rev. Appl.*, 2017, **8**, 054002.
12 K. Yamaguchi, First principles study on electronic structure of β-Ga_2O_3, *Solid State Commun.*, 2004, **131**, 739–744.
13 S. Ohira, N. Suzuki, N. Arai, M. Tanaka, T. Sugawara, K. Nakajima and T. Shishido, Characterization of transparent and conducting Sn-doped β-Ga_2O_3 single crystal after annealing, *Thin Solid Films*, 2008, **516**, 5763–5767.
14 G. Q. Pei, C. T. Xia, Y. J. Dong, B. Wu, T. Wang and J. Xu, Studies of magnetic interactions in Mn-doped β-Ga_2O_3 from first-principles calculations, *Scr. Mater.*, 2008, **58**, 943–946.
15 W. Z. Xiao, L. L. Wang, L. Xu, Q. Wan and B. S. Zou, Electronic structure and magnetic interactions in Ni-doped β-Ga_2O_3 from first-principles calculations, *Scr. Mater.*, 2009, **61**, 477–480.
16 Y. J. Zhang, J. L. Yan, G. Zhao and W. F. Xie, First-principles study on electronic structure and optical properties of Sn-doped β-Ga_2O_3, *Physica B*, 2010, **405**, 3899–3903.
17 W. Z. Xiao, L. L. Wang, L. Xu, Q. Wan and A. L. Pan, Electronic structure and magnetic properties in nitrogen-doped-Ga_2O_3 from density functional calculations, *Solid State Commun.*, 2010, **150**, 852–856.
18 A. Kumar and U. Singisetti, First principles study of thermoelectric properties of β-gallium oxide, *Appl. Phys. Lett.*, 2020, **117**, 262104.
19 Y. J. Zhang, J. L. Yan, Q. S. Li, C. Qu, L. Y. Zhang and T. Li, Structural and optical properties of N-doped β-Ga_2O_3 films deposited by RF magnetron sputtering, *Physica B*, 2011, **406**, 3079–3082.

20 Y. J. Zhang, J. L. Yan, Q. S. Li, C. Qu, L. Y. Zhang and W. F. Xie, Optical and structural properties of Cu-doped β-Ga_2O_3 films, *Mater. Sci. Eng., B*, 2011, **176**, 846–849.
21 L. Y. Zhang, J. L. Yan, Y. J. Zhang, T. Li and X. W. Ding, First-principles study on electronic structure and optical properties of N-doped p-type β-Ga_2O_3, *Sci. China: Phys., Mech. Astron.*, 2012, **55**, 19–24.
22 S. Seacat, J. L. Lyons and H. Peelaers, Orthorhombic alloys of Ga_2O_3 and Al_2O_3, *Appl. Phys. Lett.*, 2020, **116**, 232102.
23 W. S. Li, D. Saraswat, Y. Y. Long, K. Nomoto, D. Jena and H. G. Xing, Near-ideal reverse leakage current and practical maximum electric field in β-Ga_2O_3 Schottky barrier diodes, *Appl. Phys. Lett.*, 2020, **116**, 192101.
24 J. B. Varley, A. Perron, V. Lordi, D. Wickramaratne and J. L. Lyons, Prospects for n-type doping of $(Al_xGa_{1-x})_2O_3$ alloys, *Appl. Phys. Lett.*, 2020, **116**, 172104.
25 Z. A. Jian, S. Mohanty and E. Ahmadi, Deep UV-assisted capacitance-voltage characterization of post-deposition annealed Al_2O_3/β-Ga_2O_3 (001) MOSCAPs, *Appl. Phys. Lett.*, 2020, **116**, 242105.
26 S. J. Clark, M. D. Segall, C. J. Pickard, P. J. Hasnip, M. J. Probert, K. Refson and M. C. Payne, First principles methods using CASTEP, *Z. Kristallogr.*, 2005, **220**, 567–570.
27 D. Vanderbilt, Soft self-consistent pseudopotentials in a generalized eigenvalue formalism, *Phys. Rev. B: Condens. Matter Mater. Phys.*, 1990, **41**, 7892–7895.
28 S. Baroni, S. D. Gironcoli, A. D. Corso and P. Giannozzi, Phonons and related crystal properties from density-functional perturbation theory, *Rev. Mod. Phys.*, 2001, **73**, 515–562.
29 M. Marezio and J. P. Remeika, Bond lengths in the α-Ga_2O_3 structure and the high-pressure phase of $Ga_{2-x}Fe_xO_3$, *J. Chem. Phys.*, 1967, **46**, 1862–1865.
30 S. Geller, Crystal structure of β-Ga_2O_3, *J. Chem. Phys.*, 1960, **33**, 676–684.
31 H. H. Tippins, Optical absorption and photoconductivity in the band edge of β-Ga_2O_3, *Phys. Rev.*, 1965, **140**, A316–A319.
32 F. Tran and P. Blaha, Accurate band gaps of semiconductors and insulators with a semilocal exchange-correlation potential, *Phys. Rev. Lett.*, 2009, **102**, 226401.
33 M. Orita, H. Hiramatsu, H. Ohta, M. Hirano and H. Hosono, Preparation of highly conductive, deep ultraviolet transparent β-Ga_2O_3 thin film at low deposition temperatures, *Thin Solid Films*, 2002, **411**, 134–139.
34 Y. Oshima, E. G. Víllora, Y. Matsushita, S. Yamamoto and K. Shimamura, Epitaxial growth of phase-pure ε-Ga_2O_3 by halide vapor phase epitaxy, *J. Appl. Phys.*, 2015, **118**, 085301.
35 F. Boschi, M. Bosi, T. Berzina, E. Buffagni, C. Ferrari and R. Fornari, Hetero-epitaxy of β-Ga_2O_3 layers by MOCVD and ALD, *J. Cryst. Growth*, 2016, **443**, 25–30.